

Modelling of the mass sensitivity of the Love wave device in the presence of a viscous liquid

Ciaran McMullan[†], Hiren Mehta, Electra Gizeli[‡] and Christopher R Lowe

Institute of Biotechnology, University of Cambridge, Tennis Court Road, Cambridge CB2 1QT, UK

E-mail: e.gizeli@biotech.cam.ac.uk

Received 2 February 2000, in final form 21 July 2000

Abstract. This paper describes a new theoretical model for the analysis of the mass sensitivity of the Love wave device. We use this model along with calculations from perturbation theory to calculate sensitivity. The model is based on Love wave propagation in an isotropic, non-piezoelectric quartz substrate over-layered by a silica waveguiding layer and immersed in a viscous liquid. The analysis considers power flow in the three-layered system, comprising the quartz substrate, the silica over-layer and the viscous liquid. The model fully accounts for the first time for the power that flows through the liquid phase and assesses its effect on mass sensitivity. Mass sensitivity values were obtained by determining the displacement field throughout the viscous liquid and the Love waveguide device. The resulting velocity field was used to generate a number of trial functions that had solutions assuming stress and strain continuity at the boundaries, and the complex dispersion relation was evaluated numerically. The resulting wavevector k and propagation constant β values were used to calculate the power in both the Love wave device and the liquid layer and the velocity amplitude at the surface. The model predicts that the mass sensitivity of the Love wave device will increase in the presence of a viscous solution due to power flow into the liquid.

1. Introduction

The application of shear acoustic wave devices to chemical and biological sensing has recently received much attention since these waves are very sensitive to mass deposition occurring on the device's surface/liquid interface [1]. Two of the main types of shear acoustic devices are the Quartz Crystal Microbalance (QCM) and the Shear-Horizontal Surface Acoustic Wave (SH-SAW) devices. The QCM is a resonating device where the wave propagates in the bulk of the crystal at a typical operating frequency of between 5 and 15 MHz. This device can function as a mass sensor since adsorption of a thin layer of material on the device surface alters the resonant frequency of the oscillating crystal. In a gaseous environment, the thickness of the deposited layer may be deduced from the change in frequency as a function of mass deposition and based on the Sauerbrey equation [2]. In the presence of a liquid sample, the QCM responds to changes in the mass, viscosity and conductivity of the solid/liquid interface. QCMs have been used successfully as sensors in both gaseous and liquid environments [3–8]. Unfortunately,

the resonant frequency and, hence, the sensitivity of these devices is limited by the thickness of the piezoelectric crystal, which cannot be reduced below certain values without affecting the durability of the device.

An alternative to the QCM is the SH-SAW device which utilizes a pair of interdigitated transducers (IDTs) to excite and detect a surface shear horizontal wave by coupling electrical to acoustic energy and *vice versa* [1]. SAW devices can support different types of shear horizontal (SH) waves based on the geometry of the device and the cut of the piezoelectric crystal. As in the resonating device, sensing occurs following the deposition of a layer of material on the surface of the device between the emitting and detecting IDT. In all cases, the deposited layer changes the mechanical properties of the device and, thereby, alters the velocity and amplitude of the propagating wave. In the presence of a liquid sample, surface shear acoustic waves are sensitive to interfacial mass, viscoelastic and electric changes. The use of SH-SAW waves in chemical and biological sensing has been demonstrated in several applications [9–14]. Furthermore, modelling studies of the mass sensitivity of different SH-SAW waves, such as the leaky SH-SAW [15–17] and the Acoustic Plate Mode (APM) wave [9, 18] have also appeared in the literature. The majority of the theoretical models used

[†] Current address: Physics Department, Harvard University, 164 Jefferson, Cambridge, MA, USA.

[‡] Author to whom correspondence should be addressed.

to describe the effectiveness of the SH-SAW mass sensors are based on perturbation theory [19].

The Love wave device based on a waveguide geometry has been shown to be one of the most sensitive surface SH wave devices reported to date. In this configuration the Love wave is guided within an over-layer of a low shear acoustic velocity material deposited on top of the piezoelectric substrate [20, 21]. This layered structure makes the device very sensitive to mass deposition as shown both theoretically [23–29] and experimentally [24, 27, 30–34]. Of the existing theoretical models, only one takes into account the effect of the thickness of the waveguide on the mass sensitivity [24], while the majority neglect it.

In this report, we expand our initial model and provide a more complete description of the sensor's mass sensitivity of the sensor in the presence of a liquid sample. In our preliminary analysis, mass sensitivity was described as a function of the thickness of a polymer waveguide layer [24]. This was performed by assuming that total power flow could be calculated by summing the power flow through the piezoelectric substrate and the waveguide layer. Theoretical calculations were used in comparison with experimental data in air and found to be in good agreement [24]. However, in this work, no allowance was made for the presence of the viscous liquid sample, in which the device was immersed. Since most of the attractive applications for the Love wave device use liquid samples, we believe it is important to include parameters that describe the viscous liquid in the theoretical analysis. In this paper, we (1) consider a silica overlayer as the waveguiding layer, since silica would not suffer from the high acoustic losses observed with thick polymer over-layers; and (2) include the velocity profile in the liquid sample, as a function of the viscosity of the sample, and integrate it with Auld's perturbation theory to produce a more accurate mass sensitivity formula. The inclusion of the viscous sample in our calculations leads to results with interesting implications for practical systems.

2. Theory

When an oscillating electric field is applied across an IDT patterned on the upper surface of a piezoelectric crystal, an acoustic wave of identical frequency will be excited in the crystal substrate. By using a second IDT, placed on the same upper surface but at the distal end of the acoustic device, the propagating acoustic wave may be detected after being reconverted into an electrical signal.

In the case where a z -propagating Y -cut (42.5°) quartz crystal is used as the piezoelectric substrate, an SH wave known as the Surface Skimming Bulk Wave (SSBW) is excited. As the SSBW propagates from the input to the output IDT, it diffracts inside the bulk of the crystal, resulting in severe energy loss. It has been shown that by coating the piezoelectric substrate with an over-layer that has a lower shear wave velocity than quartz, the SSBW is trapped inside the over-layer and a guided Love wave is generated [20, 21]. As a result, the wave moves away from the solid quartz boundary into the waveguiding layer and, for an optimized layer thickness, maximum displacement is obtained at the free surface. When the free surface is covered in liquid,

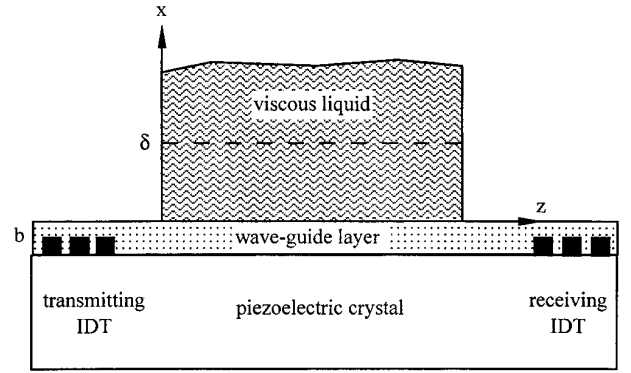


Figure 1. Schematic representation of the Love wave device. The waveguide consists of the piezoelectric quartz crystal over-layered by a silica waveguide layer of thickness, b . The excited surface skimming bulk wave (SSBW) in the piezoelectric substrate is converted in the silica over-layer to a Love wave. The penetration depth δ of the wave in the presence of liquid is also shown.

such that the device comprises a tri-layer structure (quartz, waveguiding layer and viscous liquid), the acoustic wave penetrates into the liquid and decays in amplitude away from the free surface. The penetration depth δ of the wave inside the liquid depends on the viscosity η and density ρ_l of the liquid and the operating frequency f_o of the device [22]:

$$\delta = \sqrt{\frac{\eta}{\rho_l \pi f_o}}. \quad (1)$$

A schematic representation of the Love wave system is shown in figure 1.

The guided Love wave propagating through the waveguide structure will have a propagation constant β , which is specific to the properties of the tri-layer structure. These include both the extrinsic and intrinsic properties of the system, such as the morphology, thickness, density, elasticity and viscosity of the layers. Addition of a homogeneous layer of mass on the free surface of density ρ and thickness h changes some of the values of the parameters described earlier and, thus, the characteristics of the Love wave. When the mass loading layer is very thin relative to the wavelength of the Love wave, i.e. $h \ll \lambda_{Love}$, shifts in the wave parameters may be deduced mathematically by perturbation theory [19]. Generally, the most useful way to describe quantitatively the effect of mass loading is by using the sensitivity formula S_m , which is the fractional change in a parameter of the acoustic wave as a result of mass loading divided by the value of the same parameter before mass loading, per deposited unit mass per unit area ($h\rho$). Experimentally, the most common measurement is either frequency change Δf , due to a layer of material, density ρ and thickness h loading the surface of the device and, S_m^f is defined as

$$S_m^f = \frac{1}{f_o} \lim_{h \rightarrow 0} \frac{\Delta f}{[h\rho]} \quad (2)$$

or velocity change ΔV and S_m^v is described as

$$S_m^v = \frac{1}{V_o} \lim_{h \rightarrow 0} \frac{\Delta V}{[h\rho]} \quad (3)$$

where f_o and V_o are the unperturbed frequency and phase velocity, respectively, of the acoustic wave. Both S_m^f and S_m^v

can be reconciled by using the group (V_g) and phase (V_o) velocity according to the following equation:

$$S_m^f = \frac{V_g}{V_o} S_m^v. \quad (4)$$

A more detailed expression for S_m^v was derived by Auld [19] using perturbation theory for non-piezoelectric, isotropic layered materials, and is

$$S_m^v = \frac{\Delta\beta/\beta}{[h\rho]} = \frac{\omega|v_y|_{x=b/2}^2}{4\beta P} \quad (5)$$

where $\Delta\beta$ is the change in the propagation constant β due to a thin mass loading layer of thickness h and density ρ , ω is the angular frequency, $|v_y|$ is the magnitude of the y -component (and the only non-zero component) of the velocity in the waveguide layer of thickness b and P is the total acoustic power flow through the entire trilayer structure, i.e. quartz, waveguide and liquid. The total power flow in the tri-layer system is given by

$$P = \text{Re} \left\{ \frac{1}{2} \int_{\text{cross section}} \beta(c - i\eta) \cdot |v_y|^2 dS \right\} \quad (6)$$

where η is the viscosity of the liquid and c is related to the viscosity and density of the liquid (see appendix B, equation (B3)). Qualitatively, equation (5) suggests that, not only is the sensitivity S_m^v related to angular frequency ω , which is proportional to frequency f_o , but also that it depends linearly on the square of velocity field $|v_y|^2$, which describes how the amplitude of the particle motion is distributed as the wave propagates through the tri-layer structure, and inversely on power flow (P). As one would expect, a surface sensitive guide would be one with a large surface displacement that decays rapidly with depth.

In order to use the sensitivity formula described by equation (5) the displacement field u_y of the acoustic wave in all three layers must be evaluated and its time derivative taken to give the velocity field (v_y). This is achieved by assuming that the substrate and the fluid are semi-infinite layers, hence the conditions at boundaries other than the waveguide boundary will have a negligible effect on the wave through the waveguiding layer. The nature of the contact between the layers gives rise to the boundary conditions; non-slip conditions at the boundaries are assumed, implying that there will be a continuity of displacement and shear stress across the boundaries. Thus, the displacement due to the acoustic wave in the device may be expressed as three trial functions, one for each layer, which are connected by the non-slip boundary conditions. The form of the trial function is based on the geometry of the device, and is written below.

$$\begin{array}{l} \text{fluid} \\ b/2 \\ \text{waveguiding} \\ \text{layer} \\ 0 \\ \text{substrate} \\ -b/2 \end{array} \quad \begin{array}{l} u_y^{\text{fluid}} = A e^{-(c+id)x} e^{i(\omega t - \beta z)} \quad (7a) \\ u_y^{\text{slab}} = (B e^{ikx} + D e^{-ikx}) e^{i(\omega t - \beta z)} \quad (7b) \\ u_y^{\text{sub}} = F e^{\alpha x} e^{i(\omega t - \beta z)}. \quad (7c) \end{array}$$

All the trial functions have a propagating-wave character through the $e^{i(\omega t - \beta z)}$ term while both the liquid and substrate

functions decay as the wave moves further away from the waveguiding layer. The two solid layers are assumed to behave as ideal linear elastic materials and the liquid as a Newtonian fluid obeying the Navier–Stokes equation.

By applying the boundary conditions to the trial functions, it is possible to derive a complex dispersion function $F(kb)$, given by equation (8), along with the normalized displacement field equations, equations (9a)–(9c); full derivations of these equations are given in appendix A:

$$F(kb) = \tan(kb) - \frac{(\alpha k c_{\text{sub}} c_{\text{wgl}} + ik\eta\omega(c + id)c_{\text{wgl}})}{(k^2 c_{\text{wgl}}^2 - i\alpha\eta\omega(c + id)c_{\text{sub}})} \quad (8)$$

$$u_y^{\text{liquid}} = e^{(c+id)(b/2-x)} e^{i(\omega t - \beta z)} \quad (9a)$$

$$u_y^{\text{wgl}} = \left[\cos(k(x - b/2)) - \frac{i\eta\omega(c + id)}{kc_{\text{wgl}}} \sin(k(x - b/2)) \right] \times e^{i(\omega t - \beta z)} \quad (9b)$$

$$u_y^{\text{sub}} = \left[\cos(kb) + \frac{i\eta\omega(c + id)}{kc_{\text{wgl}}} \sin(kb) \right] \times e^{(\alpha(b/2+x))} e^{i(\omega t - \beta z)}. \quad (9c)$$

By taking the time derivative of the displacement fields, equations (9a)–(9c), and then inserting them into the sensitivity formula, equation (5), it is possible to express the sensitivity of the device as a function of known parameters, i.e. the viscosity of the liquid layer η , the frequency of the wave f_o , the thickness b and the elasticity c_{wgl} of the waveguiding layer and unknown ones, such as the wavevector k , the propagation constant β , and constants c and d . However, the values for k and β may be evaluated numerically, using a complex pair root finding technique called Muller's method [35], by implementing the dispersion relation, equation (8), along with the waveguide equations below:

$$\frac{\omega^2}{(V_{\text{shear}}^{\text{wgl}})^2} = \beta^2 + k^2 \quad (10a)$$

$$V^2 = (\alpha b)^2 + (kb)^2 = (\omega b)^2 \left[\frac{1}{(V_{\text{shear}}^{\text{wgl}})^2} - \frac{1}{(V_{\text{shear}}^{\text{sub}})^2} \right]. \quad (10b)$$

The values of c and d are evaluated by inserting the liquid wavefunction into the Navier–Stokes equation details of which can be found in appendix B.

The power function in the sensitivity formula was computed by numerical integration using Simpson's method [14]. The upper limit to the power in the liquid and the lower limit to the power in the substrate were truncated such that the difference between and numerical calculation was within computational error (0.5%). This was assumed to be sufficiently accurate, given the inevitable errors associated with numerical techniques in the calculated values of β and k .

3. Results and discussion

This paper deals with the modelling of the mass sensitivity of the Love wave device in the presence of a viscous liquid. All calculations were derived for a silica over-layer and an operating frequency of 124 MHz. Perturbation theory was used to show that the wave travelling in the waveguide device

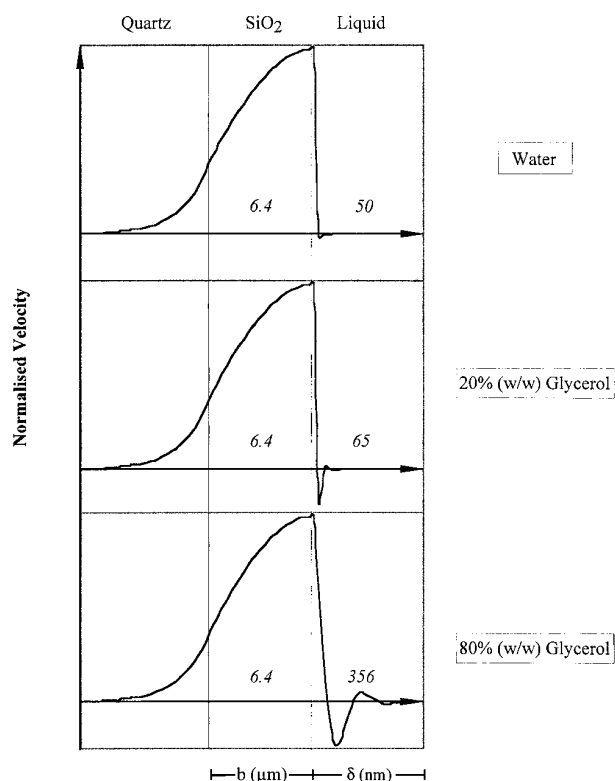


Figure 2. Real part of the velocity profile of a Love wave propagating in a SiO₂ waveguide layer in contact to water, 20 and 80% (w/w) glycerol. Velocity profiles were obtained using the expressions given by equations (A5)–(A7). The penetration depth of the Love wave in the liquid sample was calculated using equation (1). Calculations were performed for a silica thickness b of 6.4 μm and for the operating frequency f_0 of 124 MHz.

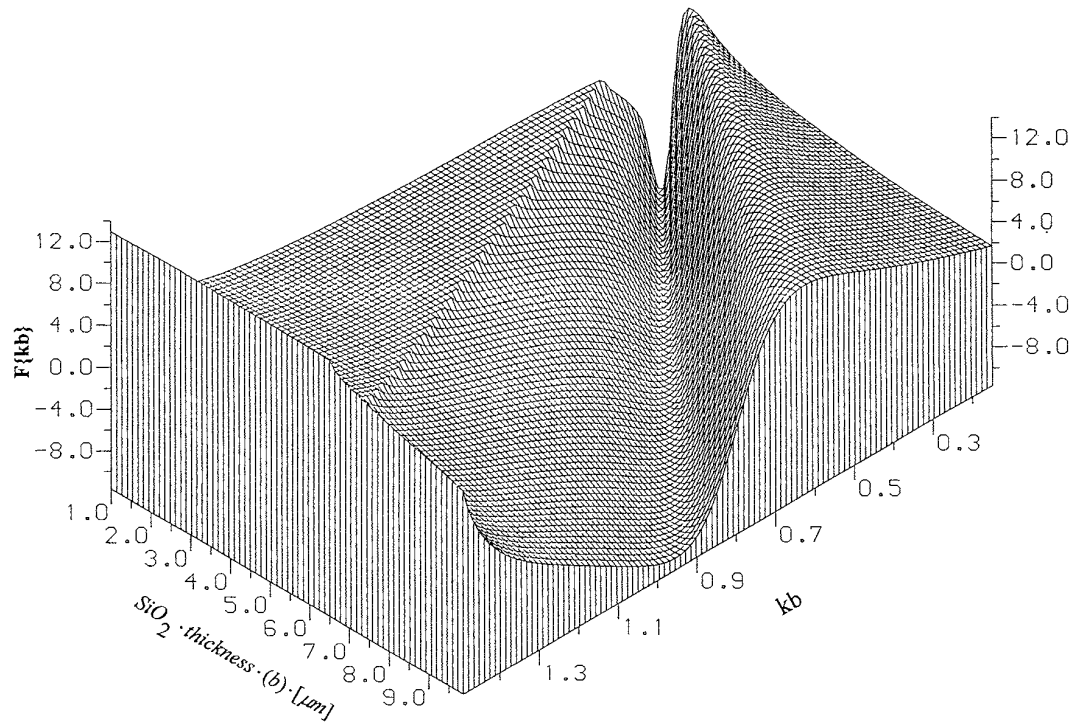
would be affected by the nature of the liquid in contact with the silica surface. This is shown with the velocity profiles of equations (A5)–(A7) where the terms c , d and α all depend upon the viscosity and density of the liquid layer (see also equations (B3) and (B4)). Figure 2 shows the velocity profile of the Love wave propagating in a silica waveguide layer when the silica surface is in contact with water, 20 and 80% (w/w) glycerol. The over-layer thickness b used in our calculations corresponded to the optimum waveguide thickness and was 6.4 μm . Assuming that the liquid is in good contact with the SiO₂ surface so that the non-slip condition is satisfied, acoustic energy will be coupled in the liquid layer. The penetration depth δ of the Love wave when the device is in contact with water, 20 and 80% (w/w) glycerol was calculated using equation (1) to be 50, 65 and 356 nm, respectively. According to figure 2, the particle displacement decreases exponentially in the waveguide structure with maximum amplitude on the silica surface for the 6.4 μm over-layer thickness. Furthermore, as the viscosity of the liquid sample increases, more energy is coupled in the viscous layer and specifically, in the area close to the waveguide surface. The deposition of a thin, elastic mass layer on the silica–liquid interface is not expected to change the distribution of the velocity profile in the three layers [14].

The propagation constant evaluated using the dispersion function, equation (8), and the waveguide expressions,

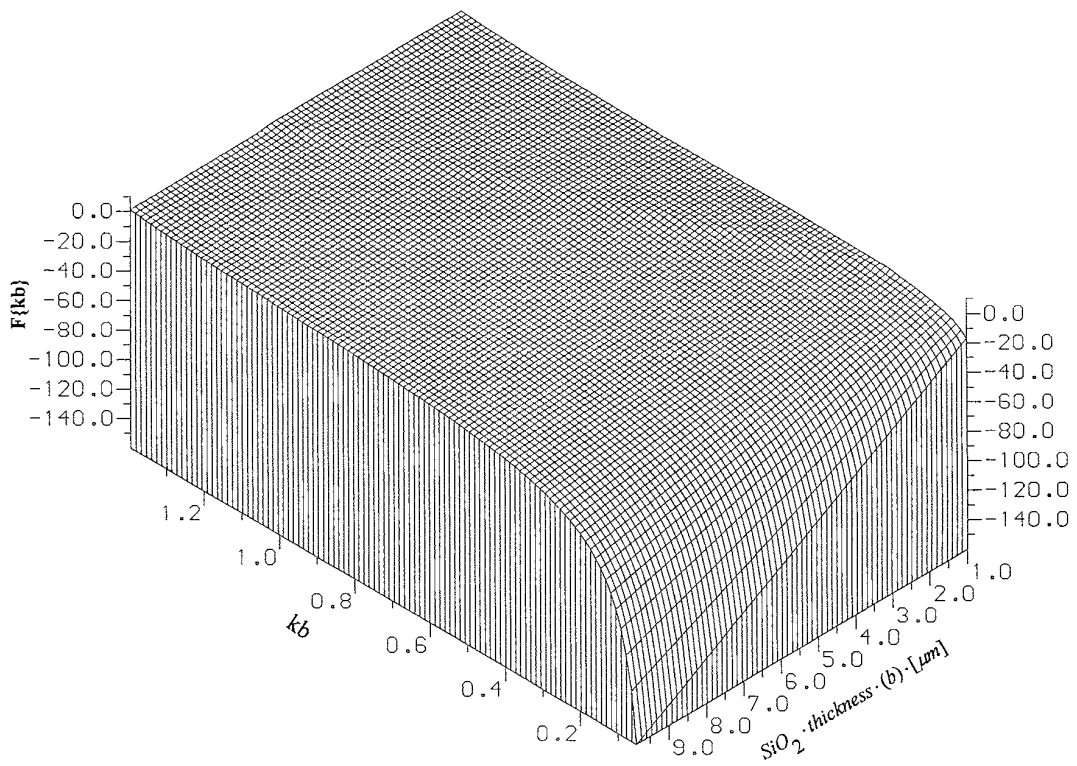
equations (10a)–(10b), must also be dependent on viscosity given that equation (8) has the viscosity term and is complex as a consequence. This is a very significant change as the complex dispersion relation is solved to give a complex propagation constant, β . It also makes the evaluation of the propagation constant using numerical root finder routines more problematic. The dispersion function, equation (8), is solved to produce the roots of wavevector k and propagation constant β . Plots of the real part of the dispersion relation, equation (8), as a function of the waveguiding layer b and κb are expressed as a 3D isometric projection in figure 3(a) and (b), for devices in contact with air and immersed in a 80% (w/w) glycerol viscous liquid, respectively. The roots to the dispersion equation lie on a plane that cuts through the origin, from which, for a particular thickness b , one can obtain the corresponding fundamental value for k . The imaginary part of the propagation constant causes an exponential decay in the wave as it propagates through the crystal. This energy loss can be attributed to viscous dissipation in the liquid. When the viscosity in the liquid is zero ($\eta = 0$), then the model reverts to the same expression described by other investigators [16] for a device in air.

Figure 4 shows the predicted sensitivity as a function of the silica over-layer thickness when the device is in contact with air, water, 20 and 80% (w/w) glycerol. Sensitivity is expressed as S_m^f since frequency is the most commonly used experimental measurement. According to figure 4, sensitivity increases with SiO₂ thickness within the range 0.5–5 μm . The maximum response to mass deposition occurs when a silica layer of approximately 6–7 μm is applied on the SSBW device surface. For over-layer thicknesses above 7 μm and below 9 μm , sensitivity drops slightly with increasing silica thickness. Figure 4 is in good agreement with theoretical results published by other investigators on the mass sensitivity of a silica-coated Love waveguide in the presence of air [29].

The effect of the liquid layer on S_m^f has been taken into account and is shown in figure 4. Generally, mass sensitivity in the presence of liquid is higher compared to that in presence of air. This is a direct result of the increase of power flow in the silica/liquid interface compared to silica/air. In addition, sensitivity to mass deposition increases with the viscosity of the liquid layer, since more acoustic energy is coupled in a glycerol solution than in water (see velocity profiles, figure 2). According to figure 4 and for a silica layer of 6.4 μm , there is almost no difference between S_m^f in water ($\eta_{\text{H}_2\text{O}} = 0.001 \text{ N s m}^{-2}$) and 20% (w/w) glycerol ($\eta_{20\%} = 0.00173 \text{ N s m}^{-2}$). The influence of the viscosity of the liquid becomes noticeable only when very viscous liquids are used, such as 80% (w/w) glycerol ($\eta_{80\%} = 0.06 \text{ N s m}^{-2}$). More specifically, it was found that the sensitivity of the device increases by less than 1% for a viscosity range between $1\text{--}2 \times 10^{-3} \text{ N s m}^{-2}$ (i.e. glycerol solutions up to 25% (w/w)). For a viscosity of 0.06 N s m^{-2} the sensitivity increases by 15%. In practice, these findings suggest that the Love wave sensor should be calibrated both to mass deposition occurring in air and liquid for gas- and liquid-based applications, respectively. Furthermore, figure 4 suggests that small variations of the viscosity of the solution, as, for example,



(a)



(b)

Figure 3. (a) Isometric projection of the dispersion function $F(kb)$ that incorporates an 80% (w/w) glycerol layer. All parameters used are similar to those in figure 2. (b) Isometric projection of the dispersion function $F(kb)$ with no fluid layer ($\eta = 0$). All data used are as in figure 2.

in the case where cell or vesicle suspensions are used, will not affect the frequency or phase response of the Love wave sensor which will still behave as a mass sensor. Although the model was derived for a Love wave sensor over-layered with

a silica layer, qualitatively, these findings should apply to all shear, surface acoustic wave sensors.

In order to derive this model, a number of assumptions were made. First, the piezoelectric and anisotropic nature of

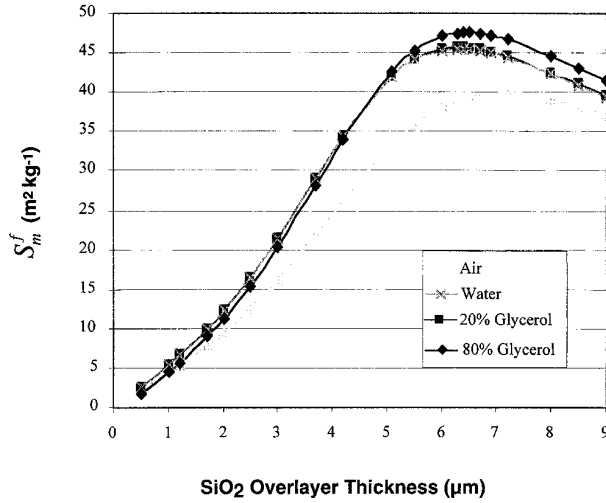


Figure 4. Plot of mass sensitivity, S_m^f , against silica layer thickness b for three liquid layers: water, 20 and 80% (w/w) glycerol. The operating frequency f_o of the Love wave device was 124 MHz.

the substrate had not been taken into account. Second, no attempt has been made to include the energy losses in the waveguide structure. The inclusion of these parameters will make the model more realistic; however, it is expected to have a small effect on our calculated mass sensitivity, as this was shown by other investigators [29]. Finally, the effect of the relaxation time of the viscous solution has not been taken into account. The latter would be expected to affect calculations concerning high viscosity glycerol solutions. For future work it is proposed to include these parameters and also apply the Muller method [35] to solve complex roots for other waveguide layers. More precise predictions for lossy over-layers and piezoelectric materials can then be determined.

4. Conclusions

In this paper we modelled the sensitivity of the Love wave to mass deposition in the presence of a viscous liquid layer by taking into account the power flow in the liquid layer using perturbation theory. Calculations were performed for a silica-coated SSBW device. It was found that mass sensitivity increased with the thickness of the silica waveguide layer for thicknesses up to 6.4 μm . Regardless of the silica thickness, the deposition of a thin elastic mass layer on the silica/liquid interface was found to affect the acoustic signal more than the deposition of the same mass on the silica/air interface. Furthermore, it was shown that mass sensitivity depends on the viscosity of the liquid sample for viscosity changes in the order of 0.06 N s m^{-2} and above. These findings clearly suggest that liquid-based Love-acoustic wave sensors will have an improved mass sensitivity compared with gas-based ones which will not be affected by small variations in the viscosity of the solution.

Appendix A

The condition of non-slip at the boundaries implies that both shear force and displacement will be continuous across

the interface. Applying these boundary conditions to the three trial wavefunctions of equations (2)–(4) results in four simultaneous equations, given as

$$Ae^{-(c+id)b/2} = Be^{ikb/2} + De^{-ikb/2} \quad (\text{A1})$$

$$Be^{-ikb/2} + De^{ikb/2} = Fe^{-ab/2} \quad (\text{A2})$$

$$\frac{-\eta(c+id)}{kc_{wgl}} \omega A e^{-(c-id)b/2} = Be^{ikb/2} - De^{-ikb/2} \quad (\text{A3})$$

$$\frac{ic_{wgl}k}{\alpha c_{sub}} (Be^{-ikb/2} - De^{ikb/2}) = Fe^{-ab/2}. \quad (\text{A4})$$

Equations (A1)–(A4) are solved to give expressions for the normalized velocity field in each of the three layers, given by equations (A5)–(A8):

$$v_y^{liquid} = e^{(c+id)(b/2-x)} \quad (\text{A5})$$

$$v_y^{wgl} = \cos(k(x-b/2)) - \frac{i\eta\omega(c+id)}{kc_{wgl}} \sin(k(x-b/2)) \quad (\text{A6})$$

$$v_y^{sub} = \left[\cos(kb) + \frac{i\eta\omega(c+id)}{kc_{wgl}} \sin(kb) \right] e^{\alpha(b/2+x)}. \quad (\text{A7})$$

The simultaneous expressions (A1)–(A4) also give the dispersion relation, equation (5).

Appendix B

The fluid overlayer is assumed to behave as a Newtonian fluid therefore obeying the Navier–Stokes equation.

$$-\nabla P^* - \eta \nabla \Delta \Omega = \rho \frac{\partial u}{\partial t} + (v \cdot \nabla)(v) \quad (\text{B1})$$

where $\Omega = \underline{\nabla} \wedge \underline{v}$.

From the geometry given earlier and assuming the wave is horizontally polarized and that

$$\underline{\nabla} P^* \approx 0 \quad \text{and} \quad \rho(\underline{v} \cdot \underline{\nabla})v \approx 0$$

equation (B1) reduces to equation (B2):

$$-\eta \left(\frac{\partial^2 v_y}{\partial x^2} + \frac{\partial^2 v_y}{\partial z^2} \right) = \rho \frac{\partial v_y}{\partial t}. \quad (\text{B2})$$

Inserting the displacement trial function for the fluid layer equation (9b) into equation (B2) and solving the latter allows both c and d to be written in terms of the real and imaginary parts of β , i.e.

$$2c^2 = \text{Im}(\beta^2) - \text{Re}(\beta^2) + [(\text{Re}(\beta^2) + \text{Im}(\beta^2))^2 + \omega\rho/\eta\{\omega\rho/\eta - 4\text{Re}(\beta)\text{Im}(\beta)\}]^{1/2} \quad (\text{B3})$$

$$2d^2 = \text{Im}(\beta^2) - \text{Re}(\beta^2) + [(\text{Re}(\beta^2) + \text{Im}(\beta^2))^2 + \omega\rho/\eta\{4\text{Re}(\beta)\text{Im}(\beta)\} - \omega\rho/\eta]^{1/2}. \quad (\text{B4})$$

Therefore, when the values of β are evaluated using the root finder the values of c and b may also be calculated.

References

- [1] Ballantine D S, White R M, Martin S J, Ricco A J, Zellers E T, Frye G C and Wohltjen H (eds) 1997 *Acoustic Wave Sensors* (New York: Academic)
- [2] Sauerbrey G Z 1959 *Z. Phys.* **155** 206–22
- [3] Nomura T and Iijima M 1981 *Anal. Chim. Acta* **131** 97–102
- [4] Kanazawa K K and Gordon J G 1985 *Anal. Chim. Acta* **175** 99–105
- [5] Edmonds T E (ed) 1988 *Chemical Sensors* (Blackie) 295–319
- [6] Su K, Williams P and Thompson M 1995 *Anal. Chem.* **67** 1010–13
- [7] Rickert J, Brecht A and Gopel W 1997 *Anal. Chem.* **69** 1441–8
- [8] Keller C A and Kasemo B 1998 *Biophys. J.* **75** 1397–402
- [9] Martin S J, Ricco A J, Niemczyk T M and Frye G C 1989 *Sensors Actuators* **20** 253–68
- [10] Kondoh J, Matsui Y and Shiokawa S 1993 *Japan. J. Appl. Phys.* **32** 2376–9
- [11] Kondoh J and Shiokawa S 1995 *Electr. Com. Jap.* **78** 54–61
- [12] Andle J C, Weaver J T, Vetelino J F and McAllister D J 1995 *Sensors Actuators* **24–25** 129–33
- [13] Kondoh J, Imayama T, Matsui Y and Shiokawa S 1996 *Electr. Com. Jap.* **79** 599–605
- [14] Weiss M, Welsch W, Schickfus M V and Hunklinger S 1998 *Anal. Chem.* **70** 2881–7
- [15] Moriizumi T, Unno Y, and Shiokawa S 1987 *IEEE Ultrason. Symp.* 579–82
- [16] Wang Z, David J, Cheeke N and Jen C K 1996 *IEEE Trans. UFFC* **43** 844–51
- [17] Kondoh J, Saito K, Shiokawa S and Suzuzki H 1996 *Japan. J. Appl. Phys.* **35** 3039–96
- [18] Josse F 1994 *Sensors Actuators A* **44** 199–208
- [19] Auld B A 1976 *Acoustic Fields and Waves in Solids* vol 2 (New York: Wiley) ch 12
- [20] Tournois P and Lardat C 1969 *IEEE Trans.* **SU-16** 107–17
- [21] Tuan H S and Ponamgi S R 1972 *IEEE Trans.* **SU-19** 9–14
- [22] Faber T E *Fluid Dynamics for Physicists* (Cambridge: Cambridge University Press)
- [23] Gizeli E, Stevenson A C, Goddard N J and Lowe C R 1992 *IEEE Trans. UFFC* **39** 657–9
- [24] Gizeli E, Stevenson A C, Goddard N J and Lowe C R 1992 *Sensors Actuators* **6** 131–7
- [25] Kovacs G and Venema A 1992 *Appl. Phys. Lett.* **61** 639–41
- [26] Gizeli E, Stevenson A C, Goddard N J and Lowe C R 1993 *Sensors Actuators B* **13** 638–9
- [27] Du J, Harding G L, Ogilvy J A, Dencher P R and Lake M 1996 *Sensors Actuators A* **56** 211–19
- [28] Jakoby B and Vellekoop M J 1997 *Smart Mater. Struct.* **6** 668–79
- [29] Ogilvy J A 1997 *J. Phys. D: Appl. Phys.* **30** 2497–501
- [30] Kovacs G, Vellekoop M J, Lubking G W and Venema A 1994 *Sensors Actuators A* **43** 43–48
- [31] Gizeli E, Lowe C R, Liley M and Vogel H 1996 *Sensors Actuators B* **34** 295–300
- [32] Gizeli E, Liley M, Lowe C R and Vogel H 1997 *Anal. Chem.* **69** 4808–13
- [33] Gizeli E 1997 *Smart Mater. Struct.* **6** 700–6
- [34] Harding G L and Du J 1997 *Smart Mater. Struct.* **6** 716–20
- [35] Press W H, Flannery B P, Teukolsky S A and Vetterling W T 1986 *Numerical Recipes* (Cambridge: Cambridge University Press) p 262